Geophys. J. Int. (2000) **142,** F1–F5

FAST-TRACK PAPER

The seismic anomaly beneath Iceland extends down to the mantle transition zone and no deeper

G. R. Foulger,[1] M. J. Pritchard,[1] B. R. Julian,[2] J. R. Evans,[2] R. M. Allen,[3] G. Nolet,[3] W. J. Morgan,[3] B. H. Bergsson,[4] P. Erlendsson,[4] S. Jakobsdóttir,[4] S. Ragnarsson,[4] R. Stefansson[4] and K. Vogfjörd[5]

[1] *Department of Geological Sciences, University of Durham, Durham,* DH1 3LE, *UK. E-mail: G.R.Foulger@durham.ac.uk*
[2] *US Geological Survey,* 345 *Middlefield Road, Menlo Park,* CA 94025, *USA*
[3] *Department of Geological and Geophysical Sciences, Guyot Hall, Princeton University, Princeton,* NJ 08544–5807, *USA*
[4] *Meteorological Office of Iceland, Bustadavegi* 9, *Reykjavik, Iceland*
[5] *National Energy Authority, Grensasvegi* 9, *Reykjavik, Iceland*

Accepted 2000 June 15. Received 2000 June 8; in original form 2000 January 26

SUMMARY

A 3-D teleseismic tomography image of the upper mantle beneath Iceland of unprecedented resolution reveals a subvertical low wave speed anomaly that is cylindrical in the upper 250 km but tabular below this. Such a morphological transition is expected towards the bottom of a buoyant upwelling. Our observations thus suggest that magmatism at the Iceland hotspot is fed by flow rising from the mantle transition zone. This result contributes to the ongoing debate about whether the upper and lower mantles convect separately or as one. The image also suggests that material flows outwards from Iceland along the Reykjanes Ridge in the upper 200 km, but is blocked in the upper 150 km beneath the Tjornes Fracture Zone. This provides direct observational support for the theory that fracture zones dam lateral flow along ridges.

Key words: fracture zones, hotspots, Iceland, magmatism, mantle transition zone.

INTRODUCTION

The opening of the north Atlantic ocean at about 54 Ma triggered massive intrusive and volcanic activity associated with the North Atlantic Volcanic Province (e.g. Vink 1984). The Iceland hotspot subsequently developed over the mid-Atlantic ridge. At Iceland a broad basalt pile rises to over 4 km above the normal level of the seafloor. It is the peak of a 1000-km-wide topographic anomaly covering much of the north Atlantic. The portion above sea level is 500×300 km in area (Fig. 1).

Magma is thought to flow outwards horizontally from beneath the hotspot southwestwards along the Reykjanes Ridge, but flow toward the Kolbeinsey Ridge to the north is thought to be blocked by the Tjornes Fracture Zone, which offsets the spreading ridge westwards by 120 km immediately north of Iceland (e.g. Sleep 1996). The whole region is associated with an extensive geoid high, anomalously thick crust (Bjarnason *et al.* 1993; Bott & Gunnarsson 1980; Du & Foulger 2000) and a geochemical anomaly (e.g. Schilling 1973).

The presence of an extensive landmass makes Iceland an important natural laboratory for studying hotspots and seeking plumes. Earlier seismic experiments detected a relatively narrow, approximately vertical, low seismic wave speed anomaly beneath Iceland (Allen *et al.* 1999; Tryggvason *et al.* 1983; Wolfe *et al.* 1997). We describe here the first results from the largest teleseismic tomography study of the upper mantle yet performed in Iceland, which reveals details of the morphology, temperature and melt distribution beneath the Iceland hotspot and the adjacent oceanic plate boundaries.

THE TOMOGRAPHY EXPERIMENT

We operated 35 three-component digital broad-band seismic stations throughout Iceland continuously from mid-1996 to mid-1998, supplementing the permanent Icelandic network (Fig. 1). The sensors were Guralp 40T, 3-CMG and 3-T broad-band seismometers. Data were logged continuously at 20 samples per second on REFTEK data loggers with 24-bit digitisers and data storage disks up to 1.2 Gbyte in size. Timing was provided by GPS, and the data were downloaded to SUN workstations.

We hand-picked the seismic phases *P*, *pP*, *PP*, *PcP*, *PKIKP*, *pPKIKP*, *S*, *sS*, *SS* and *SKS* from bandpass-filtered seismograms (0.5–2.0 Hz for *P* waves and 0.05–0.1 Hz for *S* waves)

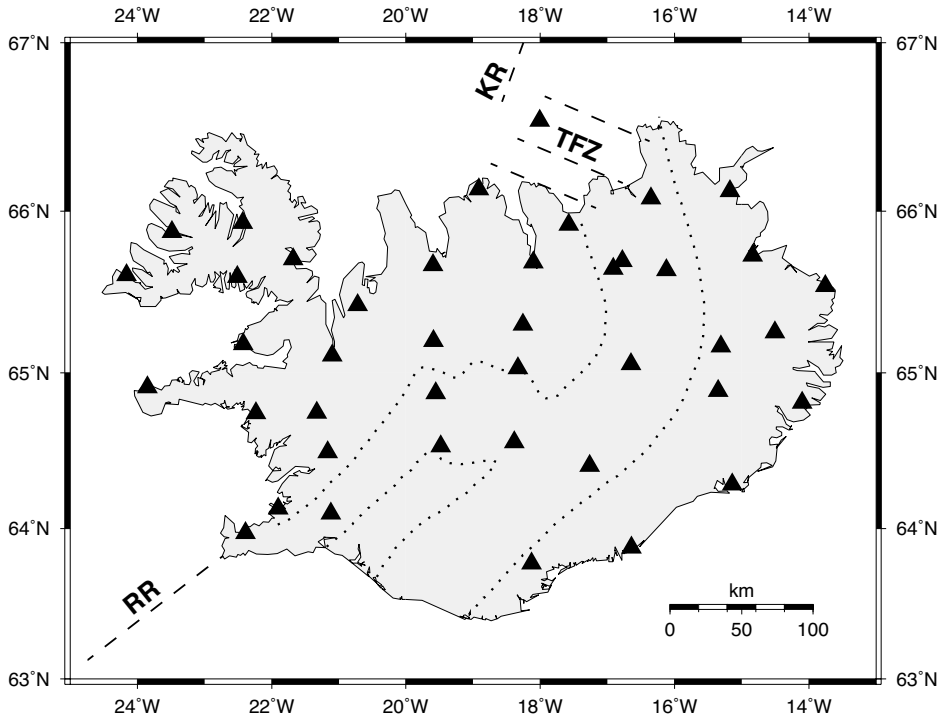

Figure 1. Map of Iceland showing the outline of the neovolcanic zone in Iceland (dotted) and all the broad-band seismic stations that provided data for our tomographic model (triangles). RR: Reykjanes Ridge; TFZ: Tjornes Fracture Zone; KR: Kolbeinsey Ridge.

for 113 well-distributed earthquakes (Fig. 2) at the 42 stations of the combined network that had broad-band sensors. We checked the times for internal consistency by comparing the patterns of arrival times from earthquakes in similar locations.

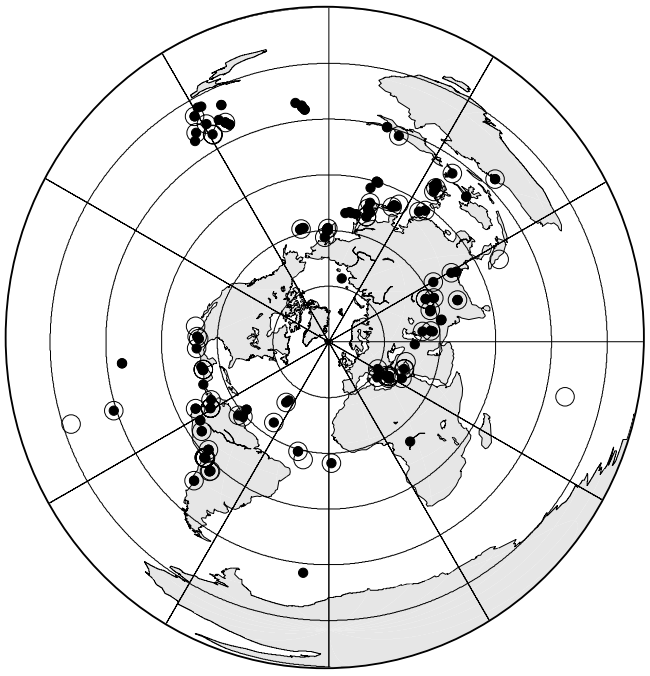

Figure 2. Earthquakes used for the tomographic inversion. Black dots: earthquakes for which compressional waves were picked; open circles: earthquakes for which shear waves were picked.

The resulting data set contains 3200 compressional and 1300 shear wave arrival times. We estimate picking accuracies to be up to about ± 0.15 s for compressional waves and ± 0.3 s for shear waves, based on the repeatability of measurements for earthquakes in hypocentral clusters.

We used the ACH tomography method (Aki *et al.* 1977) to compute independent 3-D models for the compressional and shear wave speeds (V_P and V_S) beneath Iceland. The method is non-iterative, uses straight-segment ray paths for a layered structure, represents the structure as an assemblage of blocks, each with uniform wave speed, and calculates perturbations to an initial model using damped-least-squares regularization. We used the IASP91 model as an initial model (Kennett & Engdahl 1991). The non-iterative approach is adequate for structures with wave speed anomalies that do not exceed ~ 5 per cent, which is the case for the mantle beneath Iceland. The derived models include station terms to account for structure in the upper few kilometres that is governed by local features such as central volcanoes and spreading centres and is thus highly variable across Iceland (e.g. Bjarnason *et al.* 1993; Miller *et al.* 1998).

Many suites of inversions were performed using different spatial parametrizations, damping values and data subsets, the final results being highly stable. The optimal spatial parametrization uses blocks 75×75 km in horizontal dimensions (approximately the station separation) and 50 km thick. We studied the trade-off between residual variance and the square of the Euclidean norm of the model vector for different damping parameters and selected a value of 400 s^2 per cent^{-2}, which provided a reasonable trade-off between data fit and model complexity. To reduce artefacts, to which the ACH method is prone, we used an 'offset and average' technique, and to reduce

the consequences of vertical smearing we used layer thinning (Evans & Achauer 1993, Section 13.2.3). This involves performing independent inversions with the grid offset by one half of the block size in each horizontal direction and averaging the results, and reducing layer thickness to considerably less than the station spacing (Fig. 3). Using layers significantly thinner than the nominal vertical-resolution distance (1.5–2 times the station spacing) minimizes artefacts and perceptual difficulties associated with thick layers, but does not distort or change the smearing inherent to the ray distribution (Evans & Achauer 1993). The pre-inversion rms arrival-time residuals were 0.40 s for compressional waves and 1.39 s for shear waves, relative to expected arrival times predicted by the IASP91 model. The final 3-D models produced variance reductions of 84 per cent for compressional waves and 89 per cent for shear waves.

STRUCTURE OF THE UPPER MANTLE BENEATH ICELAND

The most obvious feature in both the V_P and the V_S models is a coherent negative (slow) anomaly (Fig. 3). In the V_P model the anomaly is strongest in the top (10–58 km) layer, where the wave speed is as much as 2.7 per cent lower than in the IASP91 model. There are no crossing rays in this layer, so the structure obtained there represents the mean wave speed anomalies determined independently beneath each station. Beneath 58 km, the largest V_P anomaly is 2.1 per cent. The V_S anomaly is stronger than the V_P anomaly, with wave speed perturbations as great as 4.9 per cent.

Seismic wave speeds are sensitive to several physical and chemical effects that are expected to be important beneath hotspots and spreading ridges, including elevated temperature, partial melting, chemical depletion and olivine alignment anisotropy (e.g. Faul *et al.* 1994; Ito *et al.* 1996). The temperature anomaly is thought to be up to 200–250 °C beneath Iceland (e.g. Sleep 1990; White *et al.* 1995), which would cause variations in Vp of $\sim$1 per cent and in V_S of $\sim$1.5 per cent. The anomalies are thus consistent with a hot upwelling in the upper mantle beneath Iceland, while the strength of the V_P anomaly and the fact that the V_S anomaly is up to twice as strong suggest the presence of partial melt in a depth interval that corresponds approximately to the low-velocity zone that occupies the depth range $\sim$190–250 km (Anderson 1989).

Down to about 250 km, the V_P anomaly is approximately cylindrical, with a nearly vertical axis centred on Iceland and a radius of 100–130 km. At greater depths, and down to the limit of resolution, the anomaly is elongated north–south and underlies the spreading plate boundary in Iceland. This is well illustrated by comparing easterly cross-sections, in which the anomaly becomes narrower and weaker with depth (Fig. 3, cross-sections B–B′), to northerly cross-sections, where it widens with depth (Fig. 3, cross-sections A–A′).

The V_S image was determined independently from V_P. While it differs in detail, it is similar to the V_P image in the first-order features discussed in this paper. Although the two models were derived using similar methods, and data with similar ray geometries, the good first-order agreement between the two is consistent with the conclusion that the results are robust. A coherent low-V_S anomaly, similar in shape to the V_P anomaly, underlies Iceland at all depths. Although the V_S image is less well constrained than the V_P image, a change from an approximately cylindrical morphology in the upper 250 km to a tabular morphology, elongated in the north–south direction at greater depths, is also imaged (Fig. 3).

Close examination of the resolution matrix, including the off-diagonal terms, indicates good and highly symmetric resolution in the model to a depth of $\sim$400 km (Fig. 3). Below $\sim$450 km depth, resolution is very low beneath central Iceland. There may be slightly stronger smearing to the northeast than in other directions as a result of the uneven ray distribution (Keller *et al.* 2000; Fig. 2). The northerly orientation of the low-Vp and low-V_S features begins at 250–300 km depth and the anomaly is far less symmetric than would be expected for a simple resolution artefact under these conditions. If anything, the northerly orientation of the anomaly runs counter to any preferred smearing direction, and it is thus likely to be real.

DEPTH OF THE ANOMALY

The transition in shape that we find for the low wave speed anomaly in the upper 400 km suggests that upward flow extends no deeper than the mantle transition zone, the region between the 400 and 650 km discontinuities. Numerical models of convection from a combination of basal and internal heating predict a transition in the shape of a buoyant upwelling from tabular to cylindrical, similar to the one we observe, near the base of a convecting layer (e.g. Houseman 1990). Convection models driven by edge effects and passive upwelling beneath the ridge also predict buoyant upwellings confined to the upper mantle with the deep tabular morphology we observe (e.g. Anderson 1998; King & Anderson 1998). Such a morphology is also commonly observed in other kinds of diapirs, including salt domes and igneous intrusions, and in model experiments (Ramberg 1981). If a plume rose from the lower mantle, it would have achieved a cylindrical shape long before reaching the upper mantle.

The question of whether or not the whole mantle convects is long-standing. Several of the polymorphic transitions that are candidates for the cause of the 650 km discontinuity are endothermic (the higher-pressure phase has higher entropy), and would tend to impede whole-mantle convection because rising hot material would displace the boundary upwards. The 400 km discontinuity is exothermic, and consequently would tend to enhance convection. Comparatively small chemical differences at the 650 km discontinuity could also prevent convecting material from crossing it (Anderson 1989). Not enough is known, however, about composition, mineralogy and physical properties under the appropriate conditions for either of these arguments against whole-mantle convection to be conclusive. Our seismic results strongly suggest that the Iceland hotspot is underlain by a hot, buoyant upwelling that does not come from the lower mantle. Recent high-resolution whole-mantle tomography work (Megnin & Romanowicz 2000; Ritsema *et al.* 1999) yields a similar conclusion.

Even if this is so, however, convection in the upper and lower mantles is not expected to be independent but to be related mechanically and thermally. Buoyant upwellings in the upper mantle might tend to lie above upwellings in the lower mantle, and seismic anomalies below 650 km, which have been reported in various seismological investigations (e.g. Bijwaard & Spakman 1999; Pritchard *et al.* 2000; Shen *et al.* 1998), might thus be systematically related to convection in the upper mantle.

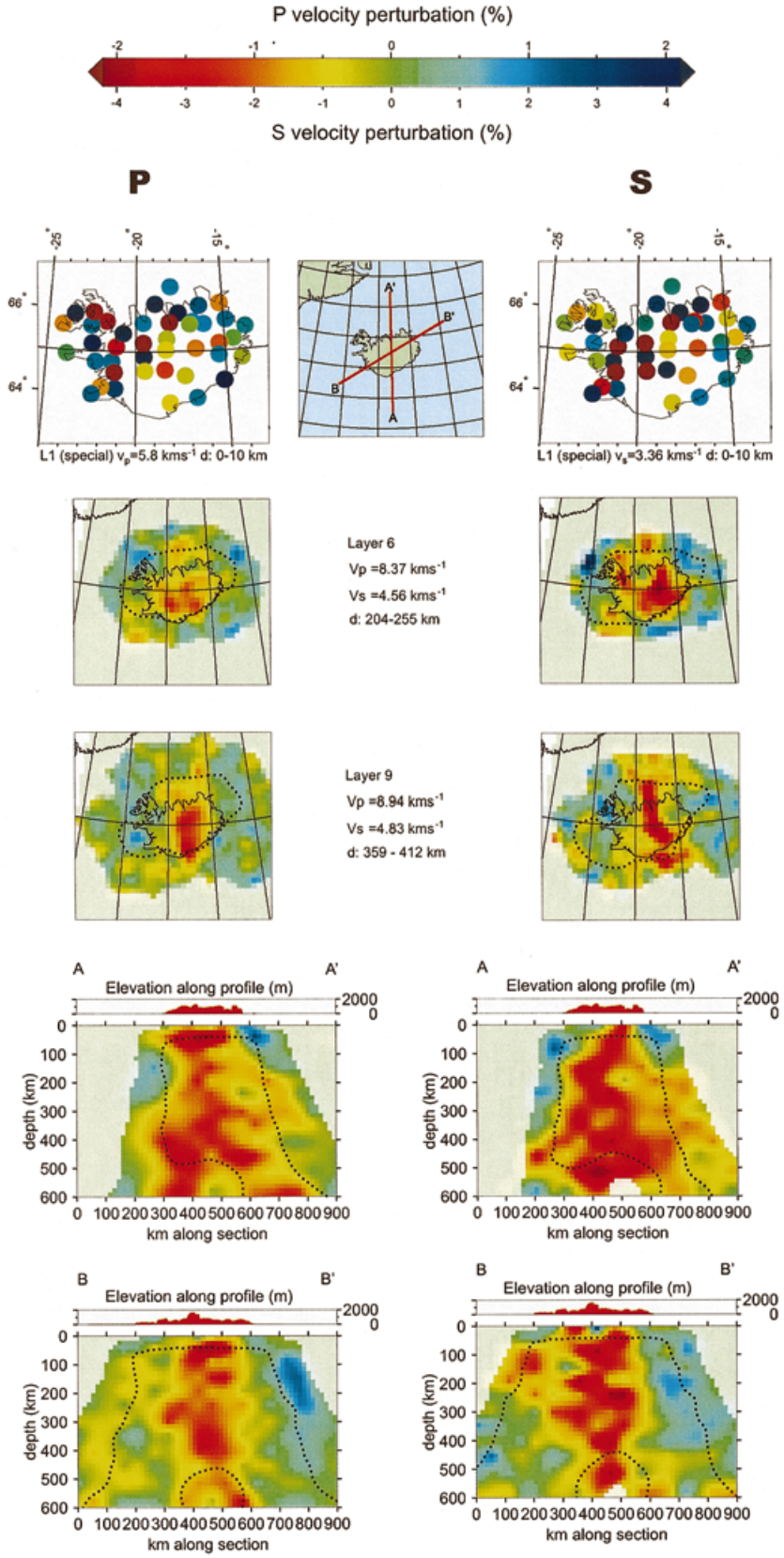

Figure 3. Variations in V_P and V_S from the IASP91 starting model for each layer, in percentage of the starting wave speed, indicated as V_P and V_S. Upper panels show wave speed anomalies in a 'special top layer' 10 km thick, which amount to station corrections. In other panels, wave speed anomalies in the original inversion blocks are interpolated at 15 km intervals using continuous curvature surface gridding (Wessel & Smith 1998) and plotted as small blocks. Each small block is approximately half the width of the offset between the original inversion blocks used in the offset-and-averaging procedure (see text; Evans & Achauer 1993). Horizontal cross-sections are shown for average perturbations in 50-km-thick layers. Small map shows the orientations of the vertical sections, which strike at 0° (A–A′) and 60° (B–B′). Dotted black line shows the contour of resolution of 0.7 for the inversion using 100-km-thick layers. Synthetic tests have shown that the equivalent resolution of layer-thinned models such as we illustrate here is effectively that of single blocks in models with layers approximately 1.5 times as thick as the station spacing (Evans & Achauer 1993).

STRUCTURE BENEATH THE SPREADING RIDGES

The ray distribution of the earthquakes and seismic stations we used yielded an image of the upper mantle under an oceanic spreading centre and a transform zone. Beneath the Reykjanes Ridge southwest of Iceland (Fig. 3, west end of cross-sections B–B′), V_P is slightly low ($\sim$0.5 per cent), whereas V_S is much lower (up to $\sim$2.4 per cent) in the depth range 50–200 km. These findings contrast with parts of the model beneath intraplate oceanic areas, where such low wave speeds are absent (e.g. Fig. 3, northeast end of cross-sections B–B′). The difference in the results for V_P and V_S below 200 km probably reflects the superior resolution in V_S in this region of the model (Fig. 3). Beneath the Tjornes Fracture Zone to the north of Iceland, low V_P and V_S wave speeds are found only below 100–150 km depth, despite excellent resolution above this depth (Fig. 3, cross sections A–A′).

The channelling of melt along ridges from hotspots (e.g. Sleep 1996) is expected to cause substantial seismic anomalies beneath the Reykjanes Ridge adjacent to Iceland. Low values of V_P are detected to $>$400 km depth and $>$100 km horizontal distance from the coast of Iceland, although this part of the model is at the edge of the well-resolved volume. These V_P lows are well supported by low values of V_S only in the depth range 50–200 km and out to $\sim$100 km from Iceland. The much stronger V_S anomaly compared with the V_P anomaly at 100–150 km beneath the Reykjanes Ridge is evidence for a small percentage of partial melt in that depth range. This may not be typical of mid-ocean ridges, but may be caused by the proximity of the Iceland hotspot. In contrast, beneath the Tjornes Fracture Zone, low V_P and V_S anomalies are not imaged in the upper 150 km, which confirms that this fracture zone acts to dam flow and provides evidence for the depth extent of the effect.

ACKNOWLEDGMENTS

This research was funded by Natural Environment Research Council (NERC) grant GST/02/1238 and NSF grant EAR 9417918. We thank the IRIS-PASSCAL instrument center for loaning the field equipment and for technical assistance. MJP was supported by a NERC studentship. Ron Girdler and two anonymous referees made many valuable suggestions that improved the manuscript.

REFERENCES

Aki, K., Christoffersson, A. & Husebye, E., 1977. Determination of the three-dimensional seismic structure of the lithosphere, *J. geophys. Res.,* **82,** 277–296.

Allen, R.M.G. *et al.*, 1999. The thin hot plume beneath Iceland, *Geophys. J. Int.,* **137,** 51–63.

Anderson, D.L., 1989. *Theory of the Earth,* Blackwell Scientific, Boston.

Anderson, D.L., 1998. The EDGES of the mantle, in *The Core–Mantle Boundary Region,* eds Gurnis, M.E., Wysession, E.K. & Buffett, B.A., pp. 255–271, AGU, Washington, DC.

Bijwaard, H. & Spakman, W., 1999. Tomographic evidence for a narrow whole mantle plume below Iceland, *Earth planet. Sci. Lett.,* **166,** 121–126.

Bjarnason, I.T., Menke, W., Flovenz, O.G. & Caress, D., 1993. Tomographic image of the mid-Atlantic plate boundary in southwestern Iceland, *J. geophys. Res.,* **98,** 6607–6622.

Bott, M.H.P. & Gunnarsson, K., 1980. Crustal structure of the Iceland–Faeroe ridge, *J. geophys. Res.,* **47,** 221–227.

Du, Z. & Foulger, G.R., 2000. Variation in the crustal structure across central Iceland, *Geophys. J. Int.,* **139,** 419–432.

Evans, J.R. & Achauer, U., 1993. Teleseismic velocity tomography using the ACH method: theory and application to continental-scale studies, in *Seismic Tomography: Theory and Applications,* eds Iyer, H.M. & Hirahara, K., pp. 319–360, Chapman & Hall, London.

Faul, U.H., Toomey, D.R. & Waff, H.S., 1994. Intergranular basaltic melt is distributed in thin, elongated inclusions, *Geophys. Res. Lett.,* **21,** 29–32.

Houseman, G.A., 1990. The thermal structure of mantle plumes: axisymmetric or triple-junction?, *Geophys. J. Int.,* **102,** 15–24.

Ito, G., Lin, J. & Gable, C.W., 1996. Dynamics of mantle flow and melting at a ridge-centered hotspot: Iceland and the mid-Atlantic ridge, *Earth planet. Sci. Lett.,* **144,** 53–74.

Keller, W.R., Anderson, D.L. & Clayton, R.W., 2000. Difficulties in seismically imaging the Icelandic hotspot, *Geophys. Res. Lett.,* submitted.

Kennett, B.L.N. & Engdahl, E.R., 1991. Travel times for global earthquake location and phase identification, *Geophys. J. Int.,* **105,** 429–466.

King, S.D. & Anderson, D.L., 1998. Edge-driven convection, *Earth planet. Sci. Lett.,* **160,** 289–296.

Megnin, C. & Romanowicz, B., 2000. The three-dimensional velocity structure of the mantle from the inversion of body, surface and higher-mode waveforms, *Geophys. J. Int.,* in press.

Miller, A.D., Julian, B.R. & Foulger, G.R., 1998. Three-dimensional seismic structure and moment tensors of non-double-couple earthquakes at the Hengill–Grensdalur volcanic complex, Iceland, *Geophys. J. Int.,* **133,** 309–325.

Pritchard, M.J., Foulger, G.R., Julian, B.R. & Fyen, J., 2000. Constraints on a plume in the mid-mantle beneath the Iceland region from seismic array data, *Geophys. J. Int.,* in press.

Ramberg, H., 1981. *Gravity, Deformation and the Earth's Crust, as Studied by Centrifuged Models,* Academic Press, London.

Ritsema, J., van Heijst, H.J. & Woodhouse, J.H., 1999. Complex shear wave velocity structure imaged beneath Africa and Iceland, *Science,* **286,** 1925–1928.

Schilling, J.-G., 1973. Iceland mantle plume: geochemical study of Reykjanes ridge, *Nature,* **242,** 565–571.

Shen, Y., Solomon, S.C., Bjarnason, I.T. & Wolfe, C.J., 1998. Seismic evidence for a lower-mantle origin of the Iceland plume, *Nature,* **395,** 62–65.

Sleep, N.H., 1990. Hotspots and mantle plumes: some phenomenology, *J. geophys. Res.,* **95,** 6715–6736.

Sleep, N.H., 1996. Lateral flow of hot plume material ponded at sublithospheric depths, *J. geophys. Res.,* **101,** 28 065–28 083.

Tryggvason, K., Husebye, E.S. & Stefánsson, R., 1983. Seismic image of the hypothesized Icelandic hot spot, *Tectonophysics,* **100,** 94–118.

Vink, G.E., 1984. A hotspot model for Iceland and the Voring Plateau, *J. geophys. Res.,* **89,** 9949–9959.

Wessel, P. & Smith, W.H.F., 1998. New, improved version of Generic Mapping Tools released, *EOS, Trans. Am. geophys. Un.,* **79,** 579.

White, R.S., Bown, J.W. & Smallwood, J.R., 1995. The temperature of the Iceland plume and origin of outward-propagating V-shaped ridges, *J. geol. Soc. Lond.,* **152,** 1039–1045.

Wolfe, C.J., Bjarnason, I.T., VanDecar, J.C. & Solomon, S.C., 1997. Seismic structure of the Iceland mantle plume, *Nature,* **385,** 245–247.